Electronic Supplementary Information (ESI)

An Unprecedent Cu$_6$ Cluster-Based Bimetallic MOF with Multiple

Open Sites for High CO$_2$ Capture and Efficient CO$_2$ Conversion

Xueyue Yu[a], Jiaming Gu[a], Baobing Tang[a], Tong Xu[a], Guanghua Li[a], Zhiyong Chang*[b, c] and Yunling Liu*[a]

[a] State Key Laboratory of Inorganic Synthesis and Preparative Chemistry, College of Chemistry, Jilin University, Changchun 130012, P. R. China

[b] Key Laboratory of Bionic Engineering, Ministry of Education, Jilin University, Changchun 130022, P. R. China

[c] College of Biological and Agricultural Engineering, Jilin University, Changchun 130022, P. R. China

E-mail: yunling@jlu.edu.cn, zychang@jlu.edu.cn

Table of Contents

S1. Calculation procedures of selectivity from IAST

The measured experimental data is excess loadings (q^{ex}) of the pure components CO_2, CH_4, C_2H_6 and C_3H_8 for **JLU-MOF108**, which should be converted to absolute loadings (q) firstly.

$$q = q^{ex} + \frac{pV_{pore}}{ZRT} \tag{1}$$

Here Z is the compressibility factor. The Peng-Robinson equation (Eq. 1) is used to estimate the value of compressibility factor to obtain the absolute loading, while the measure pore volume is also necessary.

The dual-site Langmuir-Freundlich equation (Eq. 2) is used for fitting the isotherm data at 298 K.

$$q = q_{m_1} \times \frac{b_1 \times p^{1/n_1}}{1 + b_1 \times p^{1/n_1}} + q_{m_2} \times \frac{b_2 \times p^{1/n_2}}{1 + b_2 \times p^{1/n_2}} \tag{2}$$

Here p is the pressure of the bulk gas at equilibrium with the adsorbed phase (kPa), q is the adsorbed amount per mass of adsorbent (mol kg^{-1}), q_{m1} and q_{m2} are the saturation capacities of sites 1 and 2 (mol kg^{-1}), b_1 and b_2 are the affinity coefficients of sites 1 and 2 (1/kPa), n_1 and n_2 are the deviations from an ideal homogeneous surface.

$$S = \frac{q_1/q_2}{p_1/p_2} \tag{3}$$

The selectivity of preferential adsorption of component 1 over component 2 in a mixture containing 1 and 2, perhaps in the presence of other components too, can be formally defined as q_1 and q_2 are the absolute component loadings of the adsorbed phase in the mixture. These component loadings are also termed the uptake capacities. We calculate the values of q_1 and q_2 using the Ideal Adsorbed Solution Theory (IAST) of Myers and Prausnitz (Eq. 3).

S2. Details of experiments and calculation procedures of catalytic efficiency

In a typical catalytic reaction, epoxide (20 mmol), TBAB (1 mmol, 5 mol %), activated **JLU-MOF108** (0.25 mol % open Cu sites) were put into a 15 mL Schlenk tube with solvent free environment. To activate the MOFs materials, the as-synthesized samples were activated with the exchange of methanol solvent 12 times in 2 days. After that, the samples were dried in the vacuum condition for 10 h at 70 °C and collected the MOFs for further cycloaddition reaction.

Before the reaction, pump out the air inside Schlenk tube/high pressure reactor and fill in pure CO_2. After 3 times pump-fill procedure, turn to specific conditions (1 bar, 25°C for PO and 80 °C for other epoxides in Schlenk tube). The stirring speed was 400 rpm (the speed could slow down for PO in order to reduce PO's low-boiling-point volatilization in continuous stirring). After centrifuging to recycle the catalyst, a little supernatant reaction mixture was taken to analyze by ^{1}H-NMR.

The yields of PO, 1, 2-epoxy-3-phenoxypropane, glycidyl-2-methylphenyl ether and cyclohexene oxide (H_a for epoxides and $H_{a'}$ for carbonates, respectively) catalyzed by **JLU-MOF108** were calculated according to the following equation (Eq. 4).

$$Yield(\%) = \frac{I_{H_{a'}}}{I_{H_a} + I_{H_{a'}}} \times 100\% \tag{4}$$

The yield of SO to styrene carbonate were determined by calculation of the ^{1}H NMR integrals of corresponding highlighted protons in styrene oxide (H$_a$), styrene carbonate (H$_{a'}$) and phenyl group (H$_b$-H$_f$) (from SO, styrene carbonate and other by-products) according to the following equation (Eq. 5).

$$Yield(\%) = \frac{5 \times I_{H_{a'}}}{I_{H_b - H_f}} \times 100\%$$

(5)

The calculation of TON (turnover number) and TOF (turnover frequency) values are according to the following equations:

$$TON = \frac{N_{Product}(mmol)}{N_{MOF}(mmol)}$$

$$TOF(h^{-1}) = \frac{N_{Product}(mmol)}{N_{MOF}(mmol) \times time(h)}$$

S3. Supporting Figures
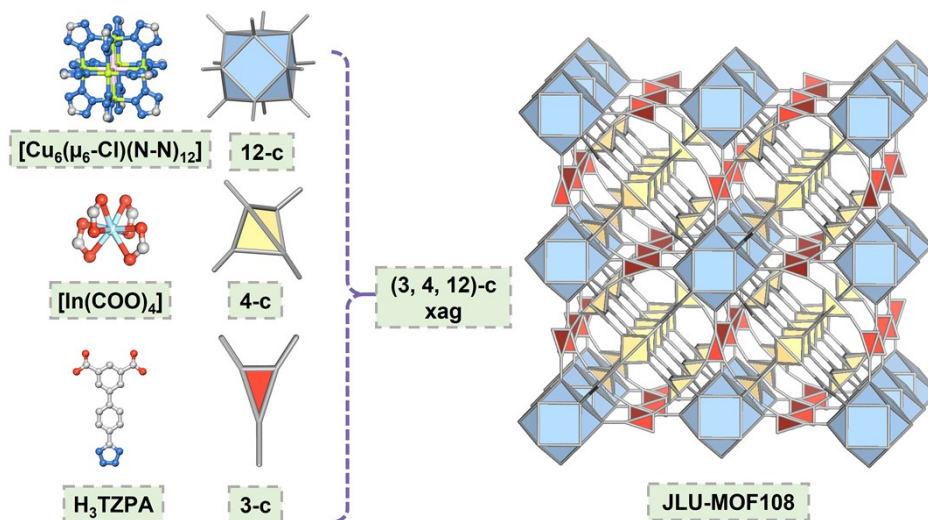
Figure S1 The hexa-nuclear copper cluster SBU and indium SBU in the structure of **JLU-MOF108**.
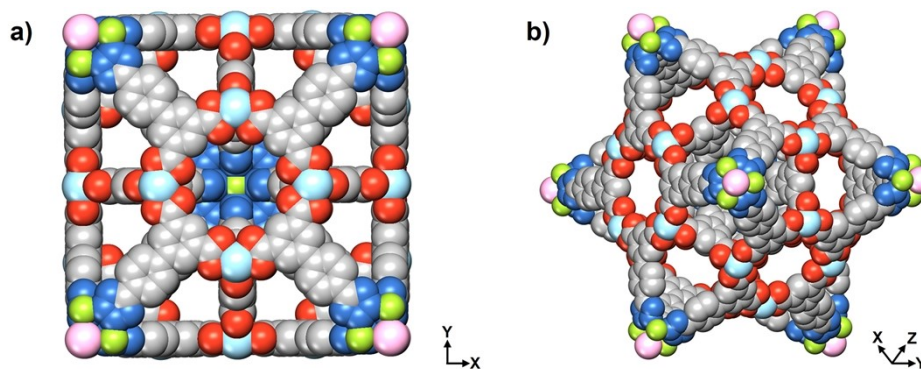
Figure S2 Space-filling view of **JLU-MOF108** with multiple pores along the [001] (a) and [111] (b) direction, respectively.
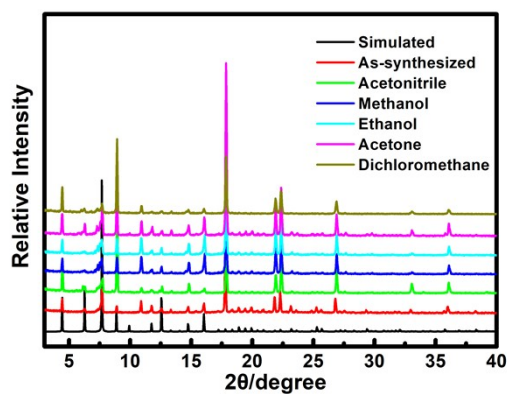
Figure S3 PXRD patterns of **JLU-MOF108** soaking in different organic solvents.
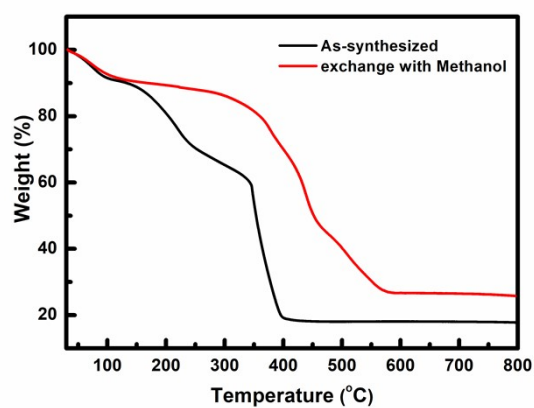
Figure S4 Thermogravimetric analysis curves of **JLU-MOF108** for the as-synthesized sample and methanol exchanged sample.
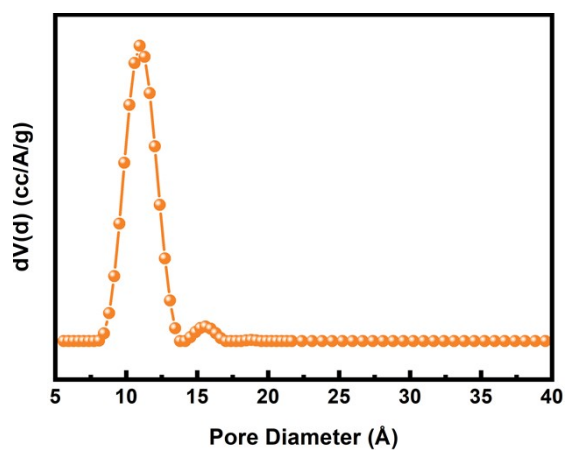
Figure S5 Pore size distribution of **JLU-MOF108**.
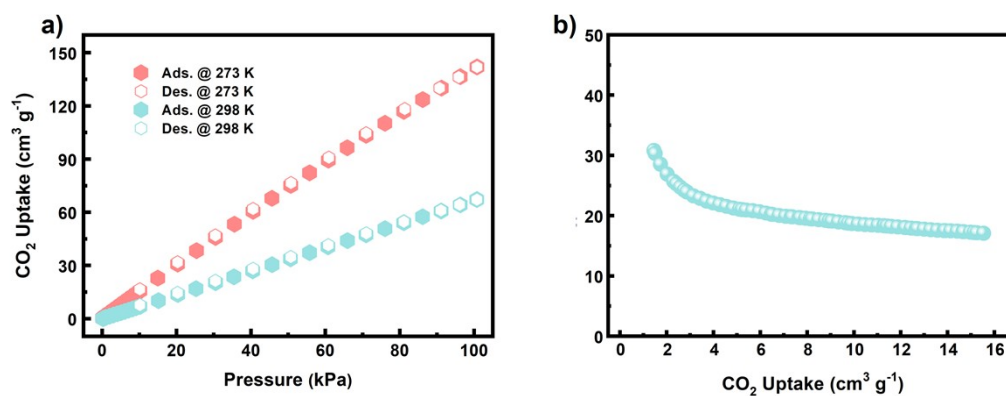
Figure S6 (a) CO_2 adsorption isotherms of **JLU-MOF108** at 273 K and 298 K; (b) Q_{st} of CO_2 for **JLU-MOF108**.
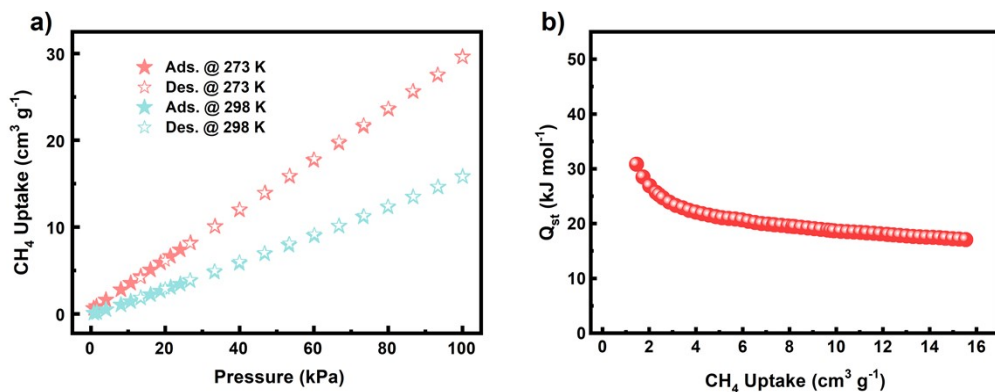
Figure S7 (a) CH$_4$ adsorption isotherms of **JLU-MOF108** at 273 K and 298 K; (b) Q_{st} of CH$_4$ for **JLU-MOF108**.
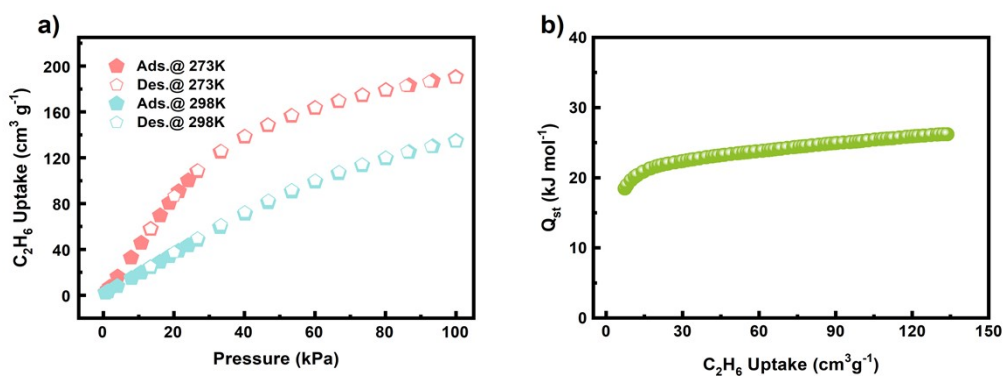
Figure S8 (a) C$_2$H$_6$ adsorption isotherms of **JLU-MOF108** at 273 K and 298 K; (b) Q_{st} of C$_2$H$_6$ for **JLU-MOF108**.
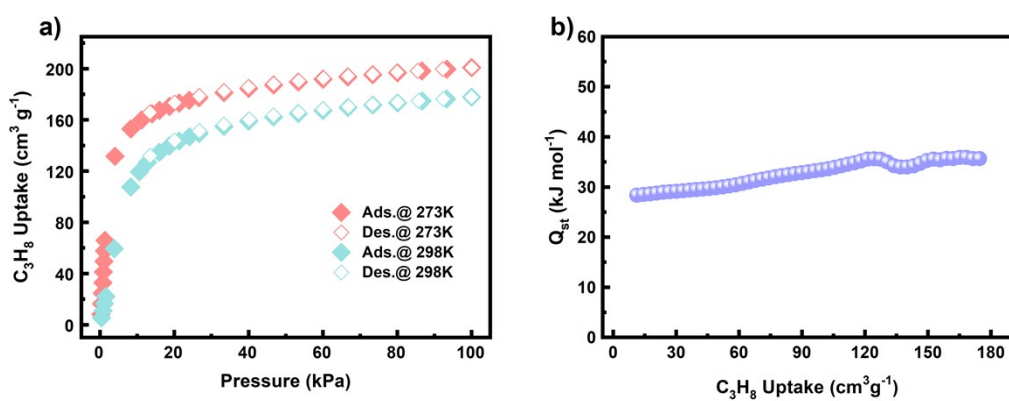
Figure S9 (a) C$_3$H$_8$ adsorption isotherms of **JLU-MOF108** at 273 K and 298 K; (b) Q_{st} of C$_3$H$_8$ for **JLU-MOF108**.
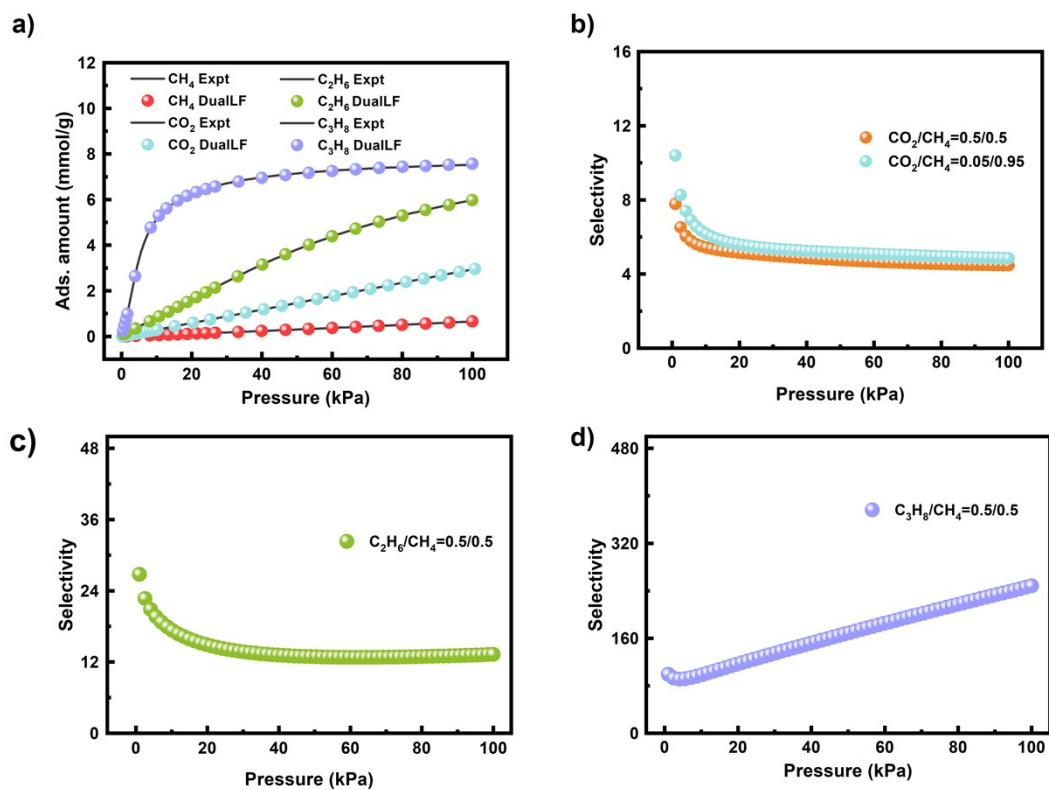
Figure S10 Gas adsorption isotherms at 298 K along with the dual-site Langmuir Freundlich (DSLF) fits (a) and adsorption selectivity predicted by the ideal adsorbed solution theory (IAST) at 298 K, 1 atm for **JLU-MOF108** (b, c and d).
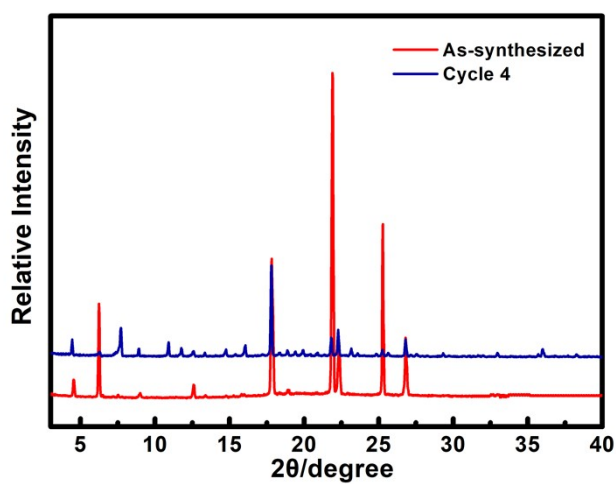
Figure S11 PXRD patterns of **JLU-MOF108** after 4 times recycled.
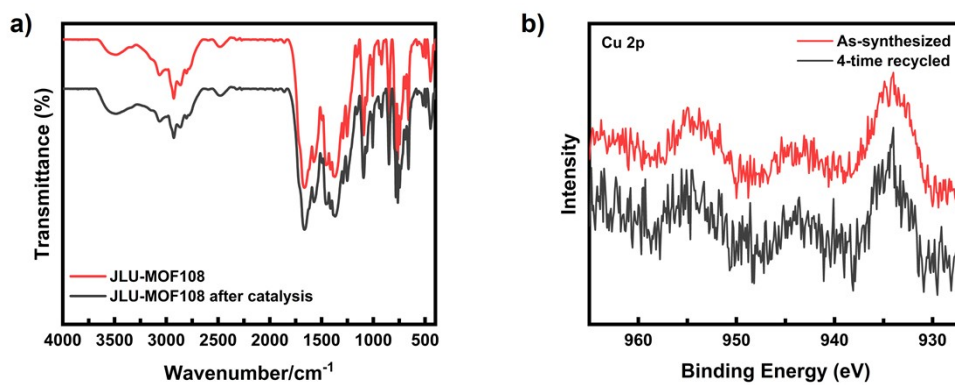
Figure S12 (a) IR spectra of **JLU-MOF108** and after 4 times recycled. (b) XPS spectraof **JLU-MOF108** and after 4 times recycled.
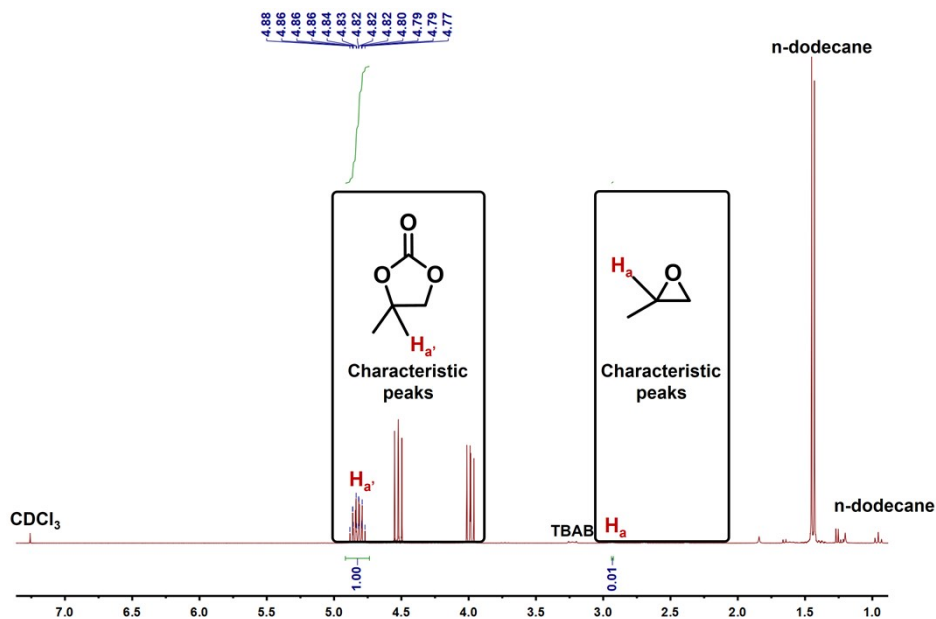
Figure S13 ^{1}H NMR spectrum of the mixture produced by cycloaddition reaction of propylene oxide catalyzed by **JLU-MOF108** in CDCl$_3$. n-dodecane was used as internal standard.
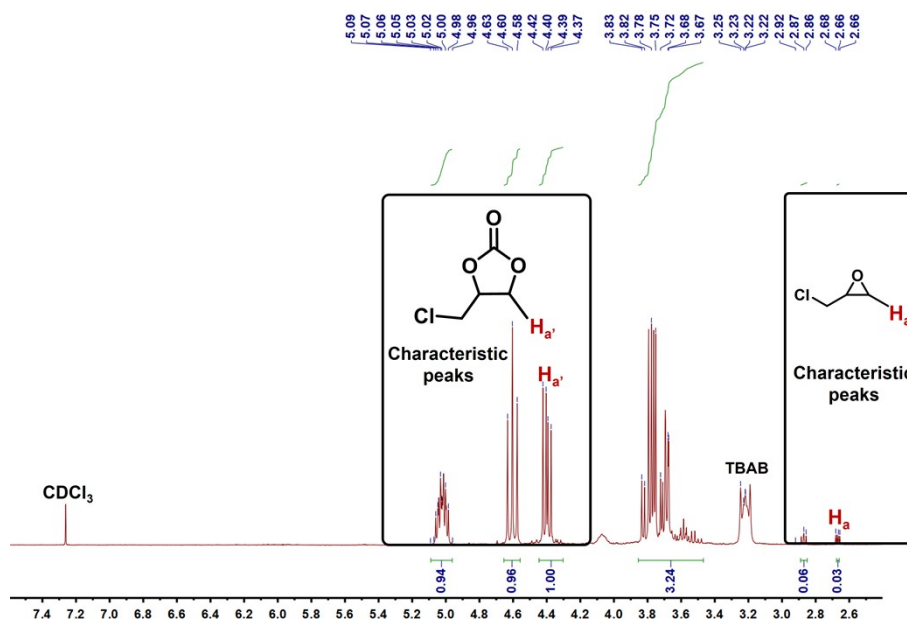
Figure S14 ^{1}H NMR spectrum of the mixture produced by cycloaddition reaction of epichlorohydrin catalyzed by **JLU-MOF108** in CDCl$_3$. n-dodecane was used as internal standard.
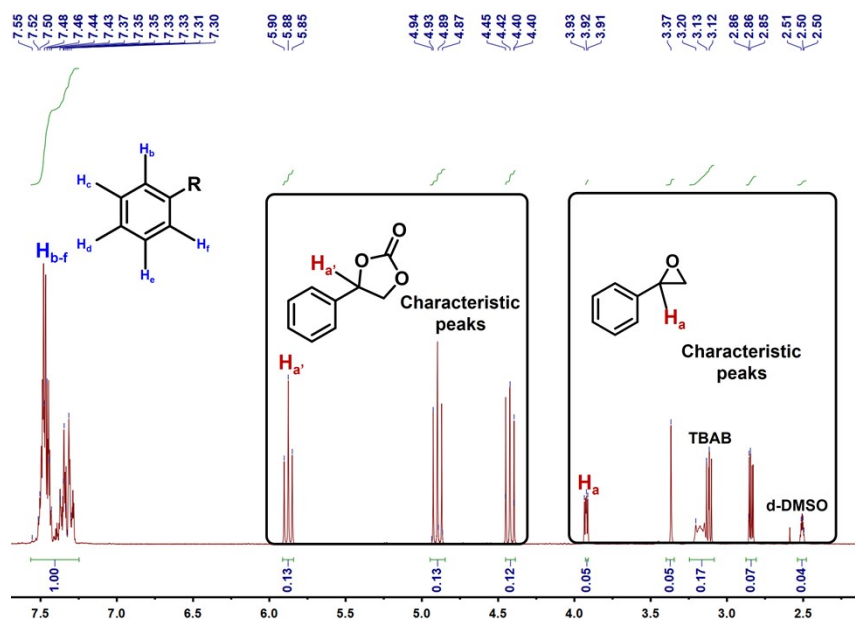
Figure S15 ^{1}H NMR spectrum of the mixture produced by cycloaddition reaction of styrene oxide catalyzed by **JLU-MOF108** in d-DMSO.
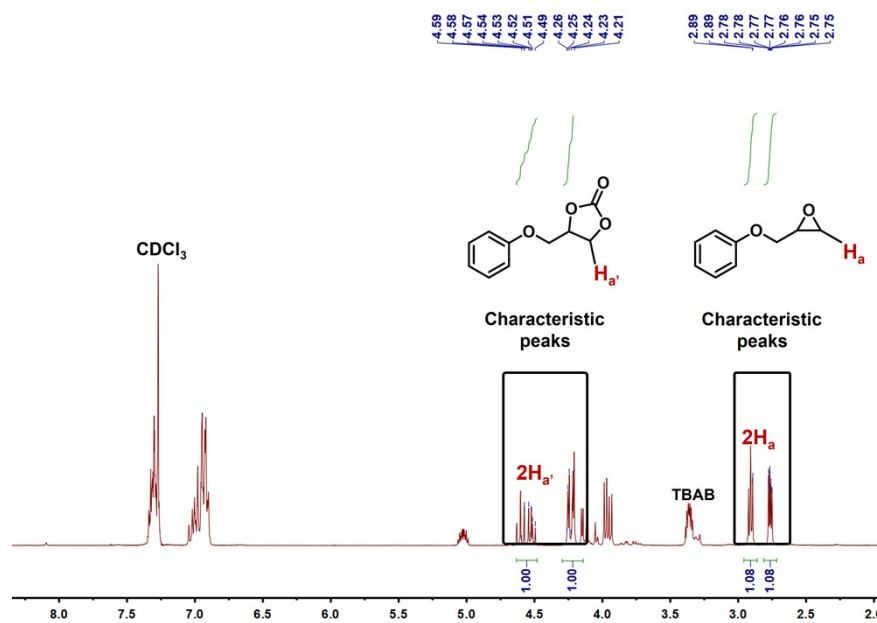
Figure S16 ^{1}H NMR spectrum of the mixture produced by cycloaddition reaction of 1, 2-epoxy-3-phenoxypropane catalyzed by **JLU-MOF108** in CDCl₃.
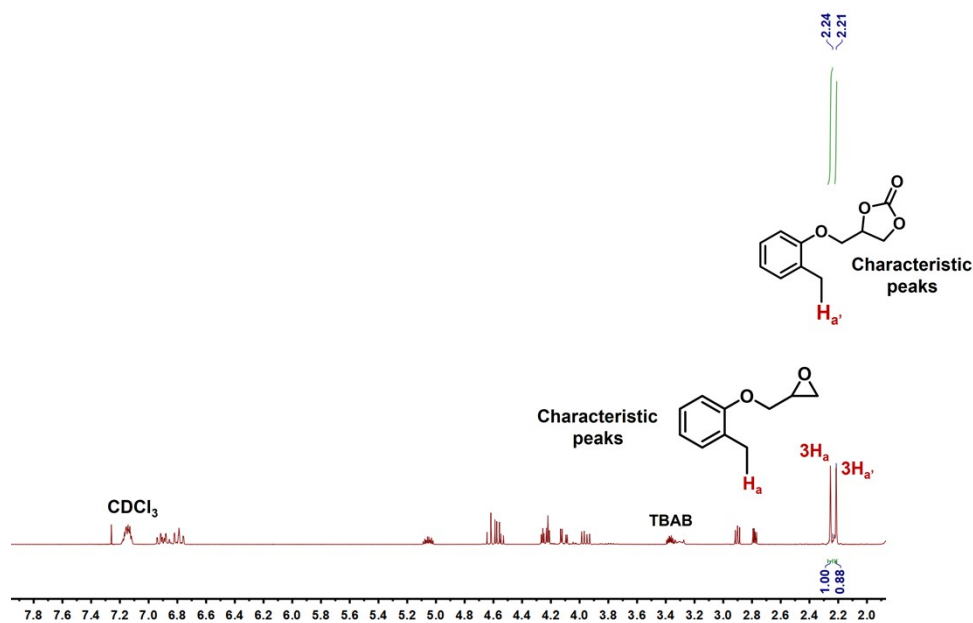
Figure S17 ^{1}H NMR spectrum of the mixture produced by cycloaddition reaction of glycidyl-2-methylphenyl ether catalyzed by **JLU-MOF108** in CDCl$_3$.
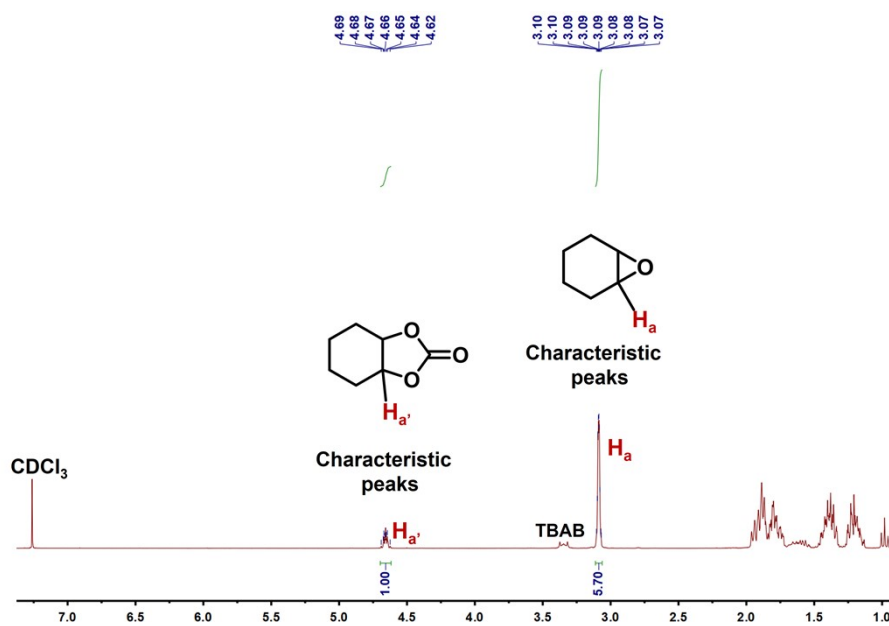
Figure S18 ^{1}H NMR spectrum of the mixture produced by cycloaddition reaction of cyclohexene oxide catalyzed by **JLU-MOF108** in CDCl$_3$.

S4. Supporting Tables

Table S1. Crystal data and structure refinements for **JLU-MOF108**.

compound	JLU-MOF108
Formula	$C_{221}H_{203}ClCu_6In_6N_{61}O_{60.5}$
Formula weight	5829.07
Temperature (K)	293(2)
Wavelength (Å)	0.71073
Crystal system	Cubic
Space group	*Im-3m*
a (Å)	28.162(3)
b (Å)	28.162(3)
c (Å)	28.162(3)
α (°)	90
β (°)	90
γ (°)	90
V (Å^3)	22335(8)
Z, D_c (Mg/m^3)	2, 0.867
$F(000)$	5892
ϑ range (deg)	1.023-25.051
reflns collected/unique	64267/1932
R_{int}	0.0612
data/restraints/params	1932/24/83
GOF on F^2	1.065
R_1, wR_2 (I>2σ(I))	0.0418, 0.1256
R_1, wR_2 (all data)	0.0503, 0.1317
CCDC No.	2338522

Table S2. Selected bond lengths [Å] and angles [°] for **JLU-MOF108**.

JLU-MOF108			
In(1)-O(2)	2.200(3)	O(2)#3-In(1)-O(1)	134.35(10)
In(1)-O(2)#1	2.200(3)	O(1)#3-In(1)-O(1)	77.98(13)
In(1)-O(2)#2	2.200(3)	O(1)#2-In(1)-O(1)	127.16(8)
In(1)-O(2)#3	2.200(3)	O(1)#1-In(1)-O(1)	127.16(8)
In(1)-O(1)#3	2.390(3)	O(2)-In(1)-C(10)#2	87.88(3)
In(1)-O(1)#2	2.390(3)	O(2)#1-In(1)-C(10)#2	162.03(13)
In(1)-O(1)#1	2.390(3)	O(2)#2-In(1)-C(10)#2	28.70(12)
In(1)-O(1)	2.390(3)	O(2)#3-In(1)-C(10)#2	87.88(3)
In(1)-C(10)#2	2.644(4)	O(1)#3-In(1)-C(10)#2	107.93(8)
In(1)-C(10)#3	2.644(4)	O(1)#2-In(1)-C(10)#2	27.67(11)
In(1)-C(10)#1	2.644(4)	O(1)#1-In(1)-C(10)#2	105.66(12)
In(1)-C(10)	2.644(4)	O(1)-In(1)-C(10)#2	107.93(8)
Cu(1)-N(2)#4	1.975(3)	O(2)-In(1)-C(10)#3	162.03(13)
Cu(1)-N(2)#5	1.975(3)	O(2)#1-In(1)-C(10)#3	87.88(3)
Cu(1)-N(2)#6	1.975(3)	O(2)#2-In(1)-C(10)#3	87.88(3)
Cu(1)-N(2)	1.975(3)	O(2)#3-In(1)-C(10)#3	28.70(12)
Cu(1)-Cl(1)	2.7176(9)	O(1)#3-In(1)-C(10)#3	27.67(11)
O(2)-In(1)-O(2)#1	90.500(15)	O(1)#2-In(1)-C(10)#3	107.93(8)
O(2)-In(1)-O(2)#2	90.500(15)	O(1)#1-In(1)-C(10)#3	107.93(8)
O(2)#1-In(1)-O(2)#2	169.28(16)	O(1)-In(1)-C(10)#3	105.66(12)
O(2)-In(1)-O(2)#3	169.28(16)	C(10)#2-In(1)-C(10)#3	99.03(7)
O(2)#1-In(1)-O(2)#3	90.500(15)	O(2)-In(1)-C(10)#1	87.88(3)
O(2)#2-In(1)-O(2)#3	90.500(15)	O(2)#1-In(1)-C(10)#1	28.70(12)
O(2)-In(1)-O(1)#3	134.35(10)	O(2)#2-In(1)-C(10)#1	162.03(13)
O(2)#1-In(1)-O(1)#3	85.83(6)	O(2)#3-In(1)-C(10)#1	87.88(3)
O(2)#2-In(1)-O(1)#3	85.83(6)	O(1)#3-In(1)-C(10)#1	107.93(8)
O(2)#3-In(1)-O(1)#3	56.37(10)	O(1)#2-In(1)-C(10)#1	105.66(12)
O(2)-In(1)-O(1)#2	85.83(6)	O(1)#1-In(1)-C(10)#1	27.67(11)
O(2)#1-In(1)-O(1)#2	134.35(10)	O(1)-In(1)-C(10)#1	107.93(8)
O(2)#2-In(1)-O(1)#2	56.37(10)	C(10)#2-In(1)-C(10)#1	133.33(19)
O(2)#3-In(1)-O(1)#2	85.83(6)	C(10)#3-In(1)-C(10)#1	99.03(7)
O(1)#3-In(1)-O(1)#2	127.16(8)	O(2)-In(1)-C(10)	28.70(12)
O(2)-In(1)-O(1)#1	85.83(6)	O(2)#1-In(1)-C(10)	87.88(3)
O(2)#1-In(1)-O(1)#1	56.37(10)	O(2)#2-In(1)-C(10)	87.88(3)
O(2)#2-In(1)-O(1)#1	134.35(10)	O(2)#3-In(1)-C(10)	162.02(13)
O(2)#3-In(1)-O(1)#1	85.83(6)	O(1)#3-In(1)-C(10)	105.65(12)
O(1)#3-In(1)-O(1)#1	127.16(8)	O(1)#2-In(1)-C(10)	107.93(8)
O(1)#2-In(1)-O(1)#1	77.98(13)	O(1)#1-In(1)-C(10)	107.93(8)
O(2)-In(1)-O(1)	56.37(10)	O(1)-In(1)-C(10)	27.67(11)
O(2)#1-In(1)-O(1)	85.83(6)	C(10)#2-In(1)-C(10)	99.03(7)
O(2)#2-In(1)-O(1)	85.83(6)	C(10)#3-In(1)-C(10)	133.33(19)

C(10)#3-In(1)-C(10)	133.33(19)	Cu(1)#10-Cl(1)-Cu(1)#13	90.0
C(10)#1-In(1)-C(10)	99.03(7)	Cu(1)#11-Cl(1)-Cu(1)#13	90.0
N(2)#4-Cu(1)-N(2)#5	170.23(19)	Cu(1)#12-Cl(1)-Cu(1)#13	90.0
N(2)#4-Cu(1)-N(2)#6	89.585(17)	Cu(1)#10-Cl(1)-Cu(1)#14	90.0
N(2)#5-Cu(1)-N(2)#6	89.584(17)	Cu(1)#11-Cl(1)-Cu(1)#14	90.0
N(2)#4-Cu(1)-N(2)	89.584(17)	Cu(1)#12-Cl(1)-Cu(1)#14	90.0
N(2)#5-Cu(1)-N(2)	89.584(17)	Cu(1)#13-Cl(1)-Cu(1)#14	180.0
N(2)#6-Cu(1)-N(2)	170.23(19)	Cu(1)#10-Cl(1)-Cu(1)	90.0
N(2)#4-Cu(1)-Cl(1)	94.89(10)	Cu(1)#11-Cl(1)-Cu(1)	90.0
N(2)#5-Cu(1)-Cl(1)	94.89(10)	Cu(1)#12-Cl(1)-Cu(1)	180.0
N(2)#6-Cu(1)-Cl(1)	94.89(10)	Cu(1)#13-Cl(1)-Cu(1)	90.0
N(2)-Cu(1)-Cl(1)	94.89(10)	Cu(1)#14-Cl(1)-Cu(1)	90.0
Cu(1)#10-Cl(1)-Cu(1)#11	180.0	C(10)-O(1)-In(1)	87.7(3)
Cu(1)#10-Cl(1)-Cu(1)#12	90.0	C(10)-O(2)-In(1)	95.4(3)
Cu(1)#11-Cl(1)-Cu(1)#12	90.0		

Symmetry transformations used to generate equivalent atoms:

#1 -z+1/2,-y+1/2,x-1/2   #2 z+1/2,-y+1/2,x-1/2   #3 x,y,-z   #4 y,x,z   #5 -y+1,-x+1,z   #6 -x+1,-y+1,z   #7 -x+1,z,y   #8 -x+1,y,z   #9 x,z,y   #10 -y+1,-z+1,-x+1   #11 y,z,x   #12 -x+1,-y+1,-z+1   #13 z,x,y   #14 -z+1,-x+1,-y+1

Table S3. Comparisons of CO_2 uptakes for selected MOFs materials (under 1 atm, at 273 K).

Compounds	273 K CO_2 uptake (mmol g^{-1})	Reference
ZJU-12	10.6	1
Cu-TDPAT	10.1	2
JLU-Liu21	9.3	3
Cu$_2$(abtc)$_3$	8.7	4
CPM-733	7.6	5
JLU-MOF107	7.6	6
JLU-Liu20	7.2	3
JLU-MOF108	6.3	This work
CPM-33a	6.1	7
IFMC	4.1	8
NH$_2$-MIL-125	4.0	9
USTC-253	3.7	10
UiO-66-AD4	3.6	11
SNU-M10	3.3	12
MAF-23	3.3	13
1	2.8	14
TMOF-1	2.2	15
SNU-5	0.9	4

Table S4. Comparisons of CO_2 uptakes for selected MOFs materials (under 1 atm, at 298 K).

Compounds	298 K CO_2 uptake (mmol g^{-1})	Reference
Li@HKUST-1	10.6	16
Ni-4PyC	8.2	17
CPO-27-Mg	7.1	18
JLU-Liu21	5.5	3
JLU-MOF107	4.7	6
JLU-MOF108	3.0	This work
SIFSIX-3-Ni	2.8	19
FS-CuBTC$_{UM}$	2.7	20
MAF-23	2.5	13
Zn-atz-oba	2.5	21
SU-101	2.4	22
JNU-2	2.2	23
TIFSIX-3-Ni	2.1	24
LIFM-210	2.0	25
ZNU-1	1.7	26
NH$_2$-MIL-53(Al)	1.5	27
F-PYMO-Cu	1.4	28

Table S5. Comparisons of some reported MOFs-based catalysts in cycloaddition reaction of CO_2 with ECH under respectively optimized conditions [a].

MOFs-based catalyst	T/°C	P/bar	t/h	Yield/%	TOF/h^{-1}	Ref.
VPI-100(Ni)	90	10	6	98	75.0	29
VPI-100(Cu)	90	10	6	95	72.6	29
PIP-Bn-Cl	100	1	3	> 99	71.9	30
Hf-VPI-100(Cu)	90	1.5	6	97	63.4	31
Hf-VPI-100(Ni)	90	1.5	6	90	58.4	31
$Zn_{0.75}Mg_{0.25}$-MOF-74	60	8	5	98	33.2	32
JLU-MOF108	80	1	12	97	32.3	This work
Compound 2	80	1	12	96	32.0	33
1	28	1	16	> 99	25.0	34
PCN-700-Me$_2$	50	1	10	92	24.2	35
Mn-MOF-1a	80	4	12	96	21.3	36
FJI-C10	60	1	24	87	20.6	37
MIL-IMAc-Br$^-$	60	5	20	89.1	19.7	38
PCP-33	80	1	12	79	13.0	39
FJI-H14	80	1	24	95	8.2	40
JLU-Liu21	80	1	48	92	7.7	41
PCP-34	80	1	12	72	6.0	39
PNU-25-NH$_2$	55	1	18	92	5.1	42
[Zn(chdc)(L)] H$_2$O	80	10	18	91	2.8	43
$Gd_7(cda)_6(HCOO)_3(OH)_6(H_2O)_8$	80	1	12	> 99	2.7	44

[a] The catalytic results about yield and TOF are according to cited references or calculated from respective crystallographic data.

Table S6. Sizes of epoxides selected for the experiments.

Epoxides	Size (Å³)
Propylene oxide	6.1 × 4.4 × 5.0
Epichlorohydrin	7.2 × 5.6 × 5.1
Styrene oxide	9.3 × 6.9 × 4.6
1,2-epoxy-3-phenoxypropane	12.5 × 7.1× 5.4
Glycidyl-2-methylphenyl ether	12.6 × 7.8 × 5.2
Cyclohexene oxide	6.5 × 7.0× 5.0

Table S7. ICP-OES analysis of Cu^{2+} and In^{3+} after the 4 times recycled reaction.

Catalyst	Cu^{2+} concentration (ppm)	In^{3+} concentration (ppm)
JLU-MOF108	0.0277	0.0124

References

1. X. Duan, Y. Cui, Y. Yang and G. Qian, A novel methoxy-decorated metal–organic framework exhibiting high acetylene and carbon dioxide storage capacities, *CrystEngComm.*, 2017, **19**, 1464-1469.

2. G. Cai, M. Ding, Q. Wu and H. L. Jiang, Encapsulating soluble active species into hollow crystalline porous capsules beyond integration of homogeneous and heterogeneous catalysis, *Natl Sci Rev.*, 2020, **7**, 37-45.

3. B. Liu, S. Yao, C. Shi, G. Li, Q. Huo and Y. Liu, Significant enhancement of gas uptake capacity and selectivity via the judicious increase of open metal sites and Lewis basic sites within two polyhedron-based metal-organic frameworks, *Chem. Commun.*, 2016, **52**, 3223-3226.

4. Y. G. Lee, H. R. Moon, Y. E. Cheon and M. P. Suh, A comparison of the H_2 sorption capacities of isostructural metal-organic frameworks with and without accessible metal sites: [Zn_2(abtc)(dmf)$_{23}$] and [Cu_2(abtc)(dmf)$_{23}$] versus [Cu_2(abtc)$_3$], *Angew. Chem. Int. Ed.*, 2008, **47**, 7741-7745.

5. Y. Wang, X. Jia, H. Yang, Y. Wang, X. Chen, A. N. Hong, J. Li, X. Bu and P. Feng, A strategy for constructing pore-space-partitioned mofs with high uptake capacity for C_2 hydrocarbons and CO_2, *Angew. Chem. Int. Ed.*, 2020, **59**, 19027-19030.

6. T. Xu, M. Jia, X. Liu, J. Li and Y. Liu, Designing multicomponent metal-organic frameworks with hierarchical structure-mimicking distribution for high CO_2 capture performance, *Inorg. Chem.*, 2022, **61**, 7663-7670.

7. X. Zhao, X. Bu, Q. G. Zhai, H. Tran and P. Feng, Pore space partition by symmetry-matching regulated ligand insertion and dramatic tuning on carbon dioxide uptake, *J. Am. Chem. Soc.*, 2015, **137**, 1396-1399.

8. J. Qin, D. Du, W. Li, J. Zhang, S. Li, Z. Su, X. Wang, Q. Xu, K. Shao and Y. Lan, N-rich zeolite-like metal–organic framework with sodalite topology: high CO_2 uptake, selective gas adsorption and efficient drug delivery, *Chem. Sci.*, 2012, 3, 2114-2118.

9. S. Kim, J. Kim, H. Kim, H. Cho and W. Ahn, Adsorption/catalytic properties of MIL-125 and NH_2-MIL-125, *Catal. Today*, 2013, **204**, 85-93.

10. Z. Jiang, H. Wang, Y. Hu, J. Lu and H. Jiang, Polar group and defect engineering in a metal-organic framework: synergistic promotion of carbon dioxide sorption and conversion, *ChemSusChem.*, 2015, **8**, 878-885.

11. D. Hong and M. Suh, Enhancing CO_2 separation ability of a metal-organic framework by post-synthetic ligand exchange with flexible aliphatic carboxylates, *Chem. Eur. J.,* 2014, **20**, 426-434.

12. H. Choi and M. Suh, Highly selective CO_2 capture in flexible 3D coordination polymer networks, *Angew. Chem. Int. Ed.,* 2009, **48**, 6865-6869.

13. P. Liao, D. Zhou, A. Zhu, L. Jiang, R. Lin, J. Zhang and X. Chen, Strong and dynamic CO_2 sorption in a flexible porous framework possessing guest chelating claws, *J. Am. Chem. Soc.*, 2012, **134**, 17380-17383.

14. G. Chakraborty, P. Das and S. Mandal, Efficient and highly selective CO_2 capture, separation, and chemical conversion under ambient conditions by a polar-group-appended copper(II) metal-organic framework, *Inorg. Chem.*, 2021, **60**, 5071-5080.

15. G. Zhang, G. Wei, Z. Liu, S. Oliver and H. Fei, A robust sulfonate-based metal–organic framework with permanent porosity for efficient CO_2 capture and conversion, *Chem. Mater.*, 2016, **28**, 6276-6281.

16. Z. Xiang, Z. Hu, D. Cao, W. Yang, J. Lu, B. Han and W. Wang, Metal-organic frameworks with incorporated carbon nanotubes: improving carbon dioxide and methane storage capacities by lithium doping, *Angew. Chem. Int. Ed.*, 2011, **50**, 491-494.

17. S. Nandi, P. Luna, T. Daff, J. Rother, M. Liu, W. Buchanan, A. Hawari, T. Woo and R. Vaidhyanathan, A single-ligand ultra-microporous MOF for precombustion CO_2 capture and hydrogen purification, *Sci. Adv.*, 2015, **1**, e1500421.

18. L. Valenzano, B. Civalleri, K. Sillar and J. Sauer, Heats of adsorption of CO and CO_2 in metal–organic frameworks: quantum mechanical study of CPO-27-M (M = Mg, Ni, Zn), *J. Phys. Chem. C.*, 2011, **115**, 21777-21784.

19. S. Mukherjee, N. Sikdar, D. O'Nolan, D. Franz, V. Gascon, A. Kumar, N. Kumar, H. Scott, D. Madden, P. Kruger, B. Space and M. Zaworotko, Trace CO_2 capture by an ultramicroporous physisorbent with low water affinity, *Sci. Adv.*, 2019, **5**, eaax9171.

20. M. Mohamed, I. Elzeny, J. Samuel, W. Xu, C. Malliakas, Y. Picard, T. Pham, L. Miller, A. Hogan, B. Space, D. Hopkinson and S. Elsaidi, Turning normal to abnormal: reversing CO_2/C_2-hydrocarbon selectivity in HKUST-1, *Adv. Funct. Mater.*, 2024, DOI: 10.1002/adfm.202312280.

21. J. Cao, S. Mukherjee, T. Pham, Y. Wang, T. Wang, T. Zhang, X. Jiang, H. Tang, K. Forrest, B. Space, M. Zaworotko and K. Chen, One-step ethylene production from a four-component gas mixture by a single physisorbent, *Nat. Commun.*, 2021, **12**, 6507.

22. C. Hao, H. Ren, H. Zhu, Y. Chi, W. Zhao, X. Liu and W. Guo, CO_2-favored metal–organic frameworks SU-101(M) (M=Bi, In, Ga, and Al) with inverse and high selectivity of CO_2 from C_2H_2 and C_2H_4, *Sep. Purif. Technol.*, 2022, 290, 120804.

23. W. Fan, S. Yuan, W. Wang, L. Feng, X. Liu, X. Zhang, X. Wang, Z. Kang, F. Dai, D. Yuan, D. Sun and H. Zhou, Optimizing Multivariate Metal-Organic Frameworks for Efficient C_2H_2/CO_2 Separation, *J Am Chem Soc.*, 2020, **142**, 8728-8737.

24. D. Madden, D. O'Nolan, K. Chen, C. Hua, A. Kumar, T. Pham, K. Forrest, B. Space, J. Perry, M. Khraisheh and M. Zaworotko, Highly selective CO_2 removal for one-step liquefied natural

gas processing by physisorbents, *Chem. Commun.*, 2019, **55**, 3219-3222.

25. L. Zhang, L. Song, L. Meng, Y. Guo, X. Zhu, L. Qin, C. Chen, X. Xiong, Z. Wei and C. Su, Anionic Ni-based metal–organic framework with Li(I) cations in the pores for efficient C_2H_2/CO_2 separation, *ACS Appl. Mater. Interfaces,* 2023, **16**, 847-852.

26. L. Wang, W. Sun, Y. Zhang, N. Xu, R. Krishna, J. Hu, Y. Jiang, Y. He and H. Xing, Interpenetration symmetry control within ultramicroporous robust boron cluster hybrid MOFs for benchmark purification of acetylene from carbon dioxide, *Angew. Chem. Int. Ed.*, 2021, **60**, 22865-22870.

27. S. Couck, J. Denayer, G. Baron, T. Remy, J. Gascon and F. Kapteijn, An amine-functionalized MIL-53 metal-organic framework with large separation power for CO_2 and CH_4, *J. Am. Chem. Soc.*, 2009, **131**, 6326-6327.

28. X. Jiang, T. Pham, J. Cao, K. Forrest, H. Wang, J. Chen, Q. Zhang and K. Chen, Molecular sieving of acetylene from ethylene in a rigid ultra-microporous metal organic framework, *Chem. Eur. J.*, 2021, **27**, 9446-9453.

29. J. Zhu, P. Usov, W. Xu, P. Celis-Salazar, S. Lin, M. Kessinger, C. Landaverde-Alvarado, M. Cai, A. May, C. Slebodnick, D. Zhu, S. Senanayake and A. Morris, A new class of metal-cyclam-based zirconium metal-organic frameworks for CO_2 adsorption and chemical fixation, *J. Am. Chem. Soc.*, 2018, **140**, 993-1003.

30. Q. Sun, Y. Jin, B. Aguila, X. Meng, S. Ma and F. S. Xiao, Porous ionic polymers as a robust and efficient platform for capture and chemical fixation of atmospheric CO_2, *ChemSusChem*, 2017, **10**, 1160-1165.

31. J. Zhu, J. Liu, Y. Machain, B. Bonnett, S. Lin, M. Cai, M. Kessinger, P. Usov, W. Xu, S. Senanayake, D. Troya, A. Esker and A. Morris, Insights into CO_2 adsorption and chemical fixation properties of VPI-100 metal–organic frameworks, *J. Mater. Chem. A*, 2018, **6**, 22195-22203.

32. Z. Gao, L. Liang, X. Zhang, P. Xu and J. Sun, Facile one-pot synthesis of Zn/Mg-MOF-74 with unsaturated coordination metal centers for efficient CO_2 adsorption and conversion to cyclic carbonates, *ACS Appl. Mater. Interfaces,* 2021, **13**, 61334-61345.

33. X. Yu, J. Gu, X. Liu, Z. Chang and Y. Liu, Exploring the Effect of Different Secondary Building Units as Lewis Acid Sites in MOF Materials for the CO_2 Cycloaddition Reaction, *Inorg. Chem.*, 2023, **62**, 11518-11527.

34. A. Gogia and S. K. Mandal, Topologically Driven Pore/Surface Engineering in a Recyclable Microporous Metal-Organic Vessel Decorated with Hydrogen-Bond Acceptors for Solvent-Free Heterogeneous Catalysis, *ACS Appl. Mater. Interfaces,* 2022, **14**, 27941-27954.

35. S. Yuan, L. Zou, H. Li, Y. Chen, J. Qin, Q. Zhang, W. Lu, M. Hall and H. Zhou, Flexible zirconium metal-organic frameworks as bioinspired switchable catalysts, *Angew. Chem. Int. Ed.*, 2016, **55**, 10776-10780.

36. Z. Xu, Y. Zhao, L. Chen, C. Zhu, P. Li, W. Gao, J. Li and X. Zhang, Thermally activated bipyridyl-based Mn-MOFs with Lewis acid-base bifunctional sites for highly efficient catalytic cycloaddition of CO_2 with epoxides and Knoevenagel condensation reactions, *Dalton. Trans.*, 2023, **52**, 3671-3681.

37. J. Liang, Y. Xie, X. Wang, Q. Wang, T. Liu, Y. Huang and R. Cao, An imidazolium-functionalized mesoporous cationic metal-organic framework for cooperative CO_2 fixation into cyclic carbonate, *Chem. Commun.*, 2018, **54**, 342-345.

38.	D. Ma, Y. Zhang, S. Jiao, J. Li, K. Liu and Z. Shi, A tri-functional metal-organic framework heterogeneous catalyst for efficient conversion of CO_2 under mild and co-catalyst free conditions, *Chem. Commun.*, 2019, **55**, 14347-14350.

39.	M. Feng, X. Zhou, X. Wang, P. Zhou, J. Wang, Z. Cheng and D. Wang, Two stable sodalite-cage-based mofs for highly gas selective capture and conversion in cycloaddition reaction, *ACS Appl. Mater. Interfaces*, 2023, **15**, 11837-11844.

40.	A. Bhardwaj, J. Kaur, M. Wuest and F. Wuest, In situ click chemistry generation of cyclooxygenase-2 inhibitors, *Nat. Commun.*, 2017, **8**, 1.

41.	J. Gu, X. Sun, X. Liu, Y. Yuan, H. Shan and Y. Liu, Highly efficient synergistic CO_2 conversion with epoxide using copper polyhedron-based MOFs with Lewis acid and base sites, *Inorg. Chem. Front.*, 2020, **7**, 4517-4526.

42.	J. Kurisingal, Y. Rachuri, Y. Gu, R. Chitumalla, S. Vuppala, J. Jang, K. Bisht, E. Suresh and D. Park, Facile green synthesis of new copper-based metal–organic frameworks: experimental and theoretical study of the CO_2 fixation reaction, *ACS Sustain. Chem. Eng.*, 2020, **8**, 10822–10832.

43.	B. Parmar, P. Patel, R. Kureshy, N. Khan and E. Suresh, Sustainable heterogeneous catalysts for CO_2 utilization by using dual ligand Zn(II) /Cd(II) metal-organic frameworks, *Chem. Eur. J.,* 2018, **24**, 15831-15839.

44.	J. Dong, P. Cui, P. F. Shi, P. Cheng and B. Zhao, Ultrastrong alkali-resisting lanthanide-zeolites assembled by [Ln_{60}] Nanocages, *J. Am. Chem. Soc.*, 2015, **137**, 15988-15991.